Jour. of Geophysics
July 2017, Vol. XXXVIII No.3
pp 187 to 197

Structural Mapping of Kutch Rift Basin from Aeromagnetic Data

P. R. Radhika, S. P. Anand and Mita Rajaram
Indian Institute of Geomagnetism, Navi Mumbai, Maharashtra
Email: aerospl@yahoo.co.uk

Abstract

Kutch basin is an east-west oriented pericratonic rift basin at the western most periphery of the Indian craton which covers almost the entire Kutch district of the state of Gujrat. The region is conspicuously featured by uplands surrounded by lowlands. No outcrop is seen within the featureless plains and consequently subsurface information is lacking for these areas. The semi-detailed high resolution aeromagnetic data collected over the Kutch rift basin, which has a uniform coverage is analyzed in the present study. The qualitative interpretation using the crustal magnetic anomaly map suggests the major trend of the anomalies to be NW-SE and E-W, which agrees with the general trend of the basin while the minor one trends in NE-SW direction. Much of the high frequency anomalies are related to exposed and subsurface basaltic flows. One important finding is the presence of trap flows to the northwest of Kutch Mainland Fault which has not been previously reported. Different edge detection techniques were applied to the aeromagnetic data for the delineation of the major and minor magnetic contacts. From combined interpretation of the edge detection techniques like analytic signal, Horizontal Gradient Magnitude (HGM) and Euler deconvolution, we have mapped fourteen lineaments some of which does not have any surface expressions i.e., they lie within the sedimentary strata or in the Rann of Kutch. Many of these lineaments may represent basement related faults that have played a crucial role in the formation of the Kutch basin and may have been reactivated many times in the past and may have manifestation up to the surface.

Keywords: Kutch, Peri-cratonic basin, Aeromagnetic data, Basaltic flows, Analytic Signal, Horizontal Gradient Magnitude, Euler deconvolution, Upward continuation

Introduction

Kutch is a major marginal rift basin formed during the breakup of Gondwanaland (Biswas 1986). It almost covers the entire Kutch district of Gujrat state. The presence of Mesozoic sedimentary successions, which can be a potential source for petroleum, and the tectonic activities that occurs periodically have constantly attracted earth scientists towards Kutch rift basin. The presence of Rann of Kutch, salt plains and wastelands make the region inaccessible for the direct geological or ground geophysical surveys and this caused a dearth of information in these provinces. Surveys performed from airborne platforms are an alternative to get uniform data coverage as well as acquiring data over inaccessible terrain such as the salt plains. Aeromagnetic method is a cost effective method compared to other geophysical methods because of its rapid rate of coverage and low cost per unit area explored. It maps the variation of Earth's magnetic field which occurs due to the distribution of magnetic minerals especially magnetite in the rocks and it reflects the susceptibility variation of the rocks (Grant, 1985). All types of rock units are magnetic but some of them wouldn't produce detectable magnetic anomalies. The aeromagnetic survey has been used for mapping of crustal magnetic anomalies and its correlation with the subsurface geology (Besmen et.al. 2013). The data acquisition has been improved vastly by the usage of high efficient optical pumping magnetometers and unlike the older times now it can detect fine structural and sedimentary details (Gunn, 1997, Nabighian, 2005). For the study of the depositional history and the architecture of a sedimentary basin aeromagnetic data analysis has proved to be a very important tool (Philips et al. 1998, Rajaram et al.2000, Betts et al. 2004, McLean et al.2008).

It helps to delineate the basement faults (Grauch & Hudson,2007) and calculate the depth to the basement surface which has a direct significance to the depositional history of a basin. Application of the aeromagnetic data for the understanding of subtle variations in the lithological constituents of the basement rocks has been well established (Kishor and Rao, 2004). Over the last decade there has been an increase in the usage of aeromagnetic data in the study of sedimentary basins especially in the context of petroleum exploration (Alagbe et.al, 2014). Delineation of structural lineaments from magnetic data is one of the basic steps in the interpretation of aeromagnetic anomalies. In this paper we discuss the aeromagnetic data collected over the Kutch rift basin with a view to investigate the subsurface structure from the observed magnetic anomalies. We present here the preliminary interpretation results of the aeromagnetic data collected over the basin which help to identify and understand the basin structure. We also make an attempt to delineate magnetic lineaments which may represent lithological contacts or faults or fractures in the sub-surface, below the sediment cover, using edge detection techniques.

General Geology and Tectonics

Kutch is an east-west oriented marginal rift basin which is lying in the western most periphery of the Indian sub-continent (Biswas 2005, Chandrasekhar & Mishra, 2002, Prasad et.al. 2010). It is widely believed that the formation of the Kutch rift basin is associated with the breakup of Gondwanaland into the Eastern and Western in the Mesozoic. In the early Cretaceous the rifting ceased in the Kutch Rift basin and shifted towards Cambay and Narmada grabens in the south, when the Kutch basin got filled with the clastics of prograding delta as the sea regressed. (Chandrasekhar & Mishra, 2002). The Kutch basin is bounded on the north by Nagar Parkar fault, south by North Kathiawar fault and east by Radhanpur-Barmer arch while towards west it extends to the continental shelf (Biswas 1987, 2005).

The basin has a distinct structure. It is asymmetric, having a tilt towards south. The topography of the Kutch basin consists of several high lands and plains which are the areas of uplifts and half grabens (Biswas, 1987). The major uplifts are the Kutch Mainland uplift, Wagad Uplift and Island Belt uplift, which includes Patcham, Khadir and Bela islands. The major bounding faults of the uplifted regions are the Kutch Mainland Fault (KMF), South Wagad Fault (SWF) and Island Belt Fault (IBF). Generalized Geology and Tectonic map of the Kutch Rift Basin redrawn from GSI (2001), Chandrasekhar & Mishra (2002) and Ngangom & Thakkar (2016) given in Fig. 1.. The primary faults, which controlled the structural evolution are trending E-W. The KMF extends up to a 100km in NW-SE orientation in the western part of the Kutch basin, and it changes its direction to E-W in the central part. The basin contains several EW to NW-SE trending major faults such as, Katrol Hill Fault (KHF), Vigodi Fault (VF), Banni Fault, and Allah Bund Fault (Biswas, 1987). In addition to these major faults and uplifts, a couple of minor NE-SW and NW-SE trending faults are cutting across the E-W tectonic setting of the basin (Kumar et.al, 2017). Two major transverse faults trending NE-SW are cutting across the Island belt fault between Bela- Khadir and Khadir- Patcham islands. These transverse faults are buried under the Rann of Kutch sediments having no surface expressions (Ngangom and Thakkar, 2016). Two NW-SE faults are present on the either side of the Patcham island, named as Kala Dongar and Gora Dongar faults. Kala Dongar fault is an extension of the IBF which is in the northern end of the Patcham island facing towards Rann of Kutch, whereas Gora Dongar fault is cutting through the Patcham Island on its southern side (Ngangom & Thakkar, 2016, Karanth and Gadhvi, 2007).

The basin is filled with Mesozoic, Tertiary and Quaternary sediments and it possess the longest record of Mesozoic sediments in western India (Biswas, 1999). The Mesozoic rift fill sediments contain late Triassic continental, middle to late Jurassic marine and late Jurassic to early Cretaceous fluvio-deltaic sediments whereas tertiary sediments comprise mainly marine shelf sediments (Biswas, 2005; Mishra, 2009). The sediment thickness varies from less than 500m in the north to nearly 4km in the south and from 200 m in the east to almost 2.5km in the west. The Mesozoic sediments, exposed in the highlands of the basin were uplifted, folded, intruded and covered by Deccan Trap basaltic flows in Late Cretaceous-Early Palaeocene time period (Biswas, 2005). Peripheral regions of the uplifts are occupied by the tertiary shallow marine sediments. Deccan volcanic lava flows are mostly tholeiitic basalt and it is largely restricted towards the southern part of the Kutch mainland, extending from Lakhpat in the west to Anjar in the east. The trap flows are notably absent in the central and northern parts of the Mainland Kutch. The thickness of the trap gradually reduces towards the north and it is absent further north of the island belt.

Most of the igneous activities are observed in the northwestern part of the Kutch Mainland Unit (KMU) and in the northern part of the Patcham uplift. Along the central region of the KM U, a succession of igneous plugs are present and those are the major feeders of the Deccan trap flows. Various forms of intrusives are exposed which are related to the rift mechanism (Karmalkar & Sharma, 2003). One of the most important features of the basin is the presence of a NNE-SSW trending meridional high. It traverses across the positive and negative elements of the basin. This subsurface high controls the sediment facies and thickness. The surface expression of this high can be observed as raised ground of Banni (Biswas 2005).

The seismic refraction and wide-angle reflection data analysis along Jakhau-Mandvi, Mandvi-Mundra, Mundra-Adesar and Hamirpur-Halvad profiles revealed a Mesozoic sedimentary sequence sandwiched between Trap and Limestone layers. The thick Mesozoic sediments in the southern Kutch is inferred as the extension of the Mesozoic sediments delineated in the northwestern Saurashtra region (Rajendraprasad et.al, 2010). Three-dimensional (3D) model using gravity data suggests that Mesozoic sediments are at a depth of about 1 km on the northern side of Kutch Mainland Fault and extends to about 3 km, and they are at a shallow depth towards north of Vigodi Fault and Katrol Hill Fault (Seshu et.al, 2016). Based on the isostatic regional gravity analysis, the crustal thickness of the region is estimated as 44 km under the SE part of KMU and Wagad uplift and 35 km along the coast. It proposes, isostatic overcompensation, which causes differential uplift and erosion, resulting vertical stress in the basin. The vertical stress along with the horizontal stress resulting from the movement of the Indian plate can be the probable reason for the frequent earthquakes observed in this region (Chandrasekhar & Mishra, 2002). Five wells have been drilled in the onshore part of the basin (dghindia.gov.in). 1 km thickness of Tertiary sediments and presence of Mesozoic sediments at least up to 3.1 km has

been indicated in the Lakhpat well. The Sanandra well has been bottomed at 3.5 km. The data shows about 0.1 km thickness of Deccan Traps and about 3.2 km thick Mesozoic sediments. On the contrary, the Suthri well data shows 525m thickness of Tertiary sediments, 591m thickness of basalt (Deccan Traps) and more than 2219m thickness of Mesozoic sediments. The Nirona well was terminated at the depth of 2224.45 m and it shows 1km thick tertiary sediments and 1.4km thick Mesozoic sediments.

Data and Methodology

Indian Institute of Geomagnetism acquired aeromagnetic data collected in 2008 over the Kutch Rift Basin by Alcock McPhar Geotech India (Pvt.) Ltd on behalf of Directorate General of Hydrocarbons, . The survey was conducted along parallel flight lines oriented in N-S direction spaced 1km apart and with 10km spaced E-W tie lines. The flight altitude has been fixed at 300m from the topography. Crustal magnetic anomaly map prepared after applying necessary corrections to the semi detailed high resolution aeromagnetic data is represented as histogram equalized shaded relief image in Fig.2 The map reveals that the area is magnetically heterogeneous. To compensate the asymmetry arising from the lower inclinations of the ambient field and to enhance the sources at relatively shallow levels, analytic signal operation was undertaken. The analytic signal or total gradient, which is independent of magnetization direction of the body and the direction of ambient field, is a combination of first order horizontal and vertical gradients of the magnetic anomaly (Nabighian, 1984). This property makes it favorable in low magnetic latitudes (Milligan and Gunn 1997). The analytic signal can be applied both in frequency and space domain. It peaks over discrete bodies as well as their edge. The amplitude of the 3d analytic signal can be derived from the three orthogonal derivatives of the magnetic field using the equation,

$$|A(x,y)| = \left[\left(\frac{dF}{dx}\right)^2 + \left(\frac{dF}{dy}\right)^2 + \left(\frac{dF}{dz}\right)^2 \right]^{1/2}$$

Where, A(x, y) is the amplitude of the analytic signal at (x, y), and F is the observed magnetic field at (x, y) (Roest et al., 1992). The amplitude of analytic signal is directly related to the amplitudes of magnetization (MacLeod et al., 1993). Since it does not depend on the magnetization direction or the inclination of the magnetic field, the two bodies having similar geometry will produce similar analytic signal.

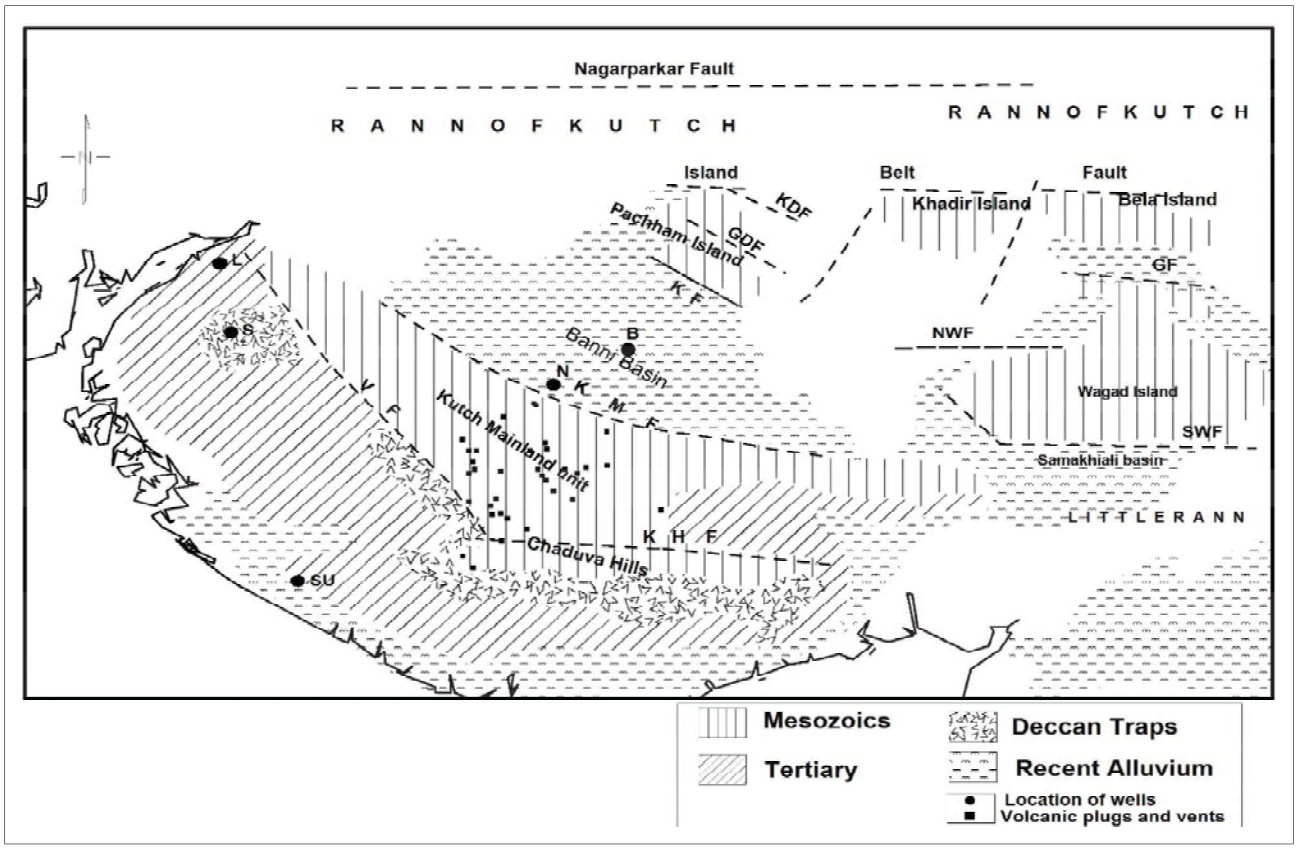

Fig 1. Geological sketch map of the Kutch rift basin: Dashed lines represent the major faults: KMF- Kutch Mainland Fault, VF- Vigodi Fault, KHF-Katrol Hill fault, MH-Median High, NWF- North Wagad Fault, SWF- South Wagad Fault, GF- Gedi Fault, KDF-Kala Dongar Fault, GDF- Gora Dongar Fault, KF-Khavda Fault. Black filled circles indicate the drilled well locations, L-Lakhpat, Su- Sutri, N- Nirona and S- Sanadra. Black squires represent the locations of volcanic plugs and vents.

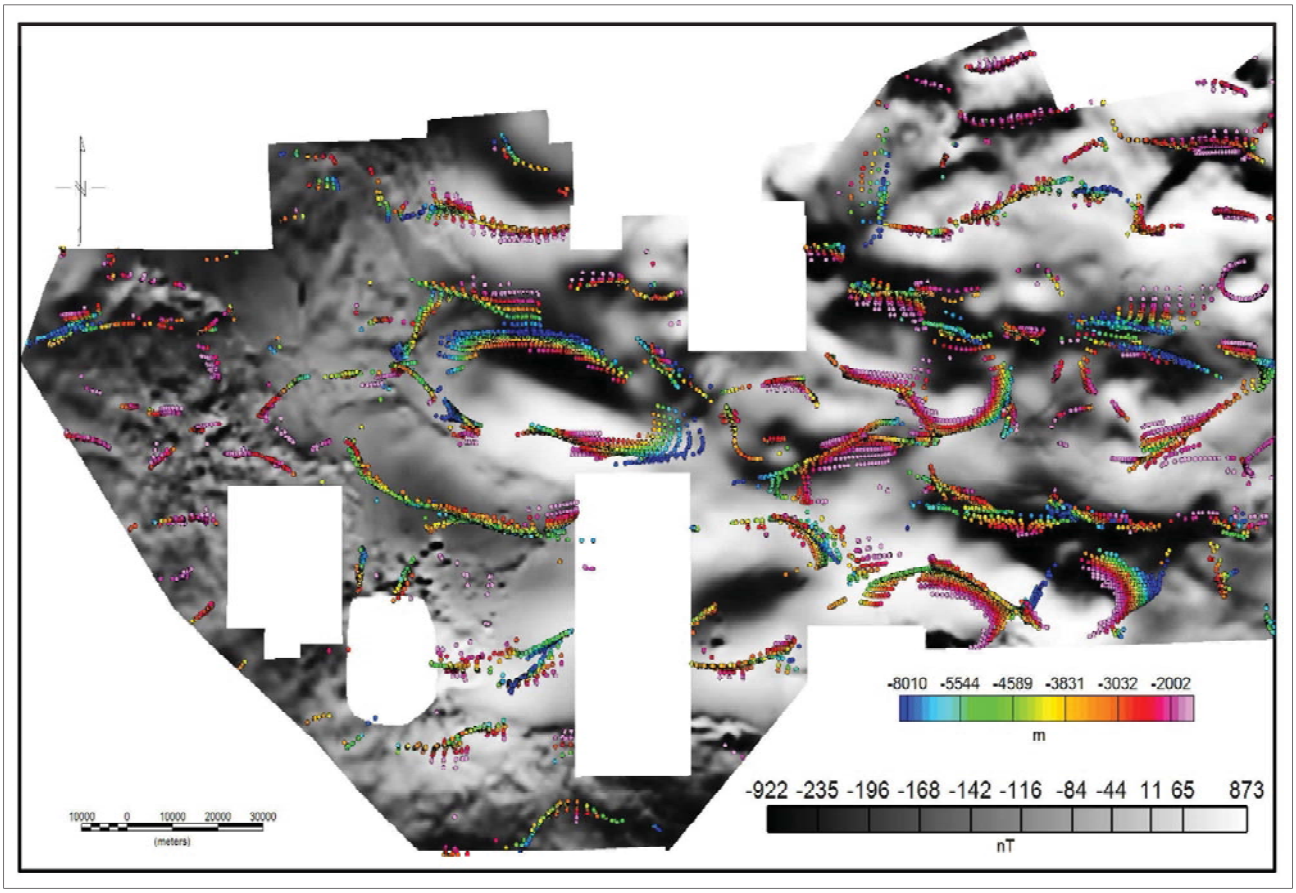

Fig. 2. Crustal Anomaly Map of the Kutch Rift Basin. Superposed is the Euler deconvolution solutions calculated using SI 0 and window length 3

To enhance the deeper and/or regional scale magnetic anomalies and attenuate the high frequency anomalies upward continuation transformation was undertaken (Blakey, 1995). The upward continuation operation smoothens the anomaly by projecting the surface mathematically upward above the datum. In the present study the data upward continued to 5km was used to calculate the HGM and Euler solution to get the contacts/lineaments at intermediate depth levels.

The estimation of the locations of the magnetic contacts, faults and other magnetic lineaments were accomplished using Horizontal Gradient Magnitude (HGM) method (Phillips, 1998). It is one of the simplest edge detection techniques available as it requires only the calculation of two first order horizontal derivatives. The calculation of the HGM demands the transformation of the anomaly map into a reduced pole grid when the region lies in a low magnetic latitude, such as the present study location and forms bipolar and asymmetric anomalies. In the present work we have used a new filter, termed Differential Reduction to Pole (DRTP) filter (Arkani-Hamed, 1988, Cooper and Cowan, 2005, Lu et al., 2003, Rajaram & Anand, 2014), which allows each grid node to have a different inclination and declination instead of an average value which is used in conventional RTP.

If M is the magnetic field, then the horizontal gradient magnitude will be given by,

$$HGM(x,y)=\sqrt{\left(\frac{\partial M}{\partial x}\right)^2+\left(\frac{\partial M}{\partial Y}\right)^2}$$

The assumptions made for this function are, the ambient magnetic field and the magnetizations are vertical, and the contacts are vertical and isolated. The local maxima of the HGM will peak above the contacts. When these assumptions get violated, the position of the maxima can be shifted away from the contacts (Grauch et.al. 2009). The first two assumptions are satisfied by using DRTP magnetic anomaly grid as input. We have calculated the HGM on the DRTP map upward continued to 5km as we are interested in regional features.

The use of Euler deconvolution applied to potential field data, for position and depth estimation of the sources, is well established (Reid 1990).The methodology for the implementation of Euler deconvolution for profile data is developed by Thompson (1982) and it is modified for gridded data by Reid (1990). For magnetic data, Euler homogeneity equation can be written in the form of

$$(x-x_0)\,dT/dx + (y-y_0)\,dT/dy + (z-z_0)\,dT/dz = N(B-T) \quad .....(1)$$

where, (x_0, y_0, z_0) is the position of a magnetic source, which has a total field T detected at (x, y, z). B is the regional value of the field and N is the degree of homogeneity which is the fall-off rate of the magnetic field, referred to as the structural index (S1) (Thompson, 1982) and it is directly related to the source shape. The unknown co-ordinates (x_0,y_0,z_0) and the regional field B, are calculated by solving the overdetermined system of linear equations by least square inversion technique. For a large grid, this can produce thousands of solutions and the better solutions will be those which forms clusters and having low relative error. The major advantage of this method is that it does not assume any particular geological model, thus, it can be applied and interpreted even when the geology cannot be properly represented by dikes or prisms and also it is independent of magnetic inclination declination and remanence.

Aeromagnetic Data Analysis

The crustal magnetic anomaly map (Fig 2) prepared after applying all the necessary corrections was employed for the qualitative interpretation. In practical terms the aeromagnetic surveys map the distribution of magnetic minerals in the crust which cause magnetic anomalies due to their high magnetic susceptibility values or remanent magnetizations (Reeves, 2005). Globally, the most abundant magnetic mineral is magnetite whose distribution in the crust is mapped in the aeromagnetic surveys. (Grant, 1985). Areas of strong positive anomalies indicate the presence of higher concentration of magnetic minerals and broad low anomalies indicate either low concentration of magnetic minerals or thick non-magnetic cover. The crustal magnetic anomaly map (Fig.2) reveals combination of NW-SE, EW and NE-SW trends which is partly in accordance with the geological and tectonic framework of the basin. By and large, basin is characterized by long to moderate wavelength anomalies with large amplitudes ranging from approximately -900nT to 900nT suggesting presence of mafic to ultramafic magnetic sources. The wavelength of the anomalies provide clues on the depth of burial of the magnetic source bodies. The long wavelength anomalies suggest the deeper/regional depth of burial and short wavelength anomalies depicts shallower and younger sources. The central part of the basin, the Banni plain/basin, covered by Tertiary sediments & salt panes and devoid of any surface exposures, displays long wavelength anomalies, indicating the presence of thick sediments and deeper sources. The southern and southwestern part of the map depicts complex magnetic variations with high frequency, high-amplitude anomalies over the exposed trap flows. Similar high frequency anomalies are not present in the central (Kutch Mainland Unit and Banni Basin) and eastern part of the basin. The Rann of Kutch region at the north eastern part of the basin, above Island belt fault, an inaccessible salt marsh, interestingly shows moderate to short wavelength anomalies. The moderate and long wavelength anomalies show high amplitudes whereas the anomalies of the exposed trap shows amplitude diversity. In general, the regions where sediment thickness is large exhibit subdued anomalies.

Since the study region lies in the low magnetic latitudes, having inclination ranging from 34.60 to 370 the spatial relationship of the total field anomaly to its source is complicated. Presence of the high amplitude bipolar anomalies can be observed in the Banni plains, which could be caused by well-defined source bodies. In the absence of remanence and with magnetic inclinations such as observed in Kutch rift basin, the positive peak of the bipolar anomalies should be located on the south and the negative peak on the north of the source with both peaks possessing almost similar amplitudes. A similar type of anomaly, with almost equal magnitudes for both the southern positive lob and northern negative lob can be observed in the Banni basin. The analytic signal method is used to simplify the interpretation by placing the anomaly peaks directly above the magnetic sources. Fig.3 shows the analytic signal map draped on the topographic map of the region. We have also superposed the previously mapped (from Fig.1) faults over the analytic signal map. The analytic signal map (Fig.3) is not completely different from the crustal anomaly map. It has made the high frequency anomalies (at shallow levels) clearer and sharper and brought the indistinct anomalies in to focus. The high frequency anomalies related to the exposed trap regions are very well delineated in the analytic signal map. The surface geology of the Kutch basin shows the presence of tholeiitic trap flows in two patches; one where Suthri well is located and other near Chavuda hills. Analytic signal map shows high frequency anomalies along the entire stretch, south of the Vigodi fault. In addition, high frequency anomalies resembling the anomaly of the exposed trap flows are present in the region, northwest of the Kutch Mainland fault (denoted ‘a’ in Fig.3) within the Rann of Kutch, indicating the possible presence of the trap flows beneath the sedimentary cover. Electrical conductivity mapping carried out using Geomagnetic Depth Sounding have shown high conductivity anomaly in this region whose conductivity is very similar to the conductivity over exposed traps, south of Vigodi fault. One of the possible explanations provided for this high conductivity is aqueous fluids released by recrystallizing magmatic intrusive bodies (Rao, et al, 2014). This gives support to our inference of the existence of basaltic flows below the Rann of Kutch. The anomalies having long wavelengths and lower amplitudes are indistinct in the map. The remarkable variations in the nature of anomalies on the either side of the major magnetic contacts are well evident in the analytic signal map. The signatures of the major faults like Kutch Mainland Fault, Vigodi fault, South Wagad fault and Island Belt fault are apparent in the map. The long wavelength anomalies those were present in the Banni basin region are diminished in amplitudes which, signifies deeper burial of the sources underneath the sedimentary cover. To the north of the Island Belt Fault, particularly in the Rann of

Kutch region, the presence of moderate wavelength features are clearly observed which indicates the occurrence of magnetic sources at very shallow depth levels.

Edge Detection for Lineament Mapping

The placement of locations of the magnetic contacts, faults and other magnetic lineaments are achieved by comparing the HGM, Euler 3D and analytic signal map. As discussed in the previous section, in the HGM assumptions about the ambient field and the nature of the lithological contacts is made, violation of these assumptions results in displacement of the location of the contacts. The advantage of the analytic signal method is that it is independent of the magnetization direction and the direction of Earth's magnetic field. For shallow sources wherever the positions of the lineaments that are displayed in the HGM has a shift from the lineaments delineated from the analytic signal map, we have taken the positions given by the analytic signal map. The HGM maxima of the magnetic anomaly map were used to delineate the common structural trends in the study area. The HGM maxima shows that the major anomalies are lying in the NW-SE direction. The signatures of the major faults in the region are well observable from the map. The HGM helps to delineate subsurface faults and contacts that have no surface expressions.

The aeromagnetic data has uniform coverage which helps for the structural and lithological mapping and it also carries the information about the depth to the top of the magnetic source bodies which makes it a very important tool in the study of depositional history and architecture of sedimentary basins. In the present study, Euler deconvolution method is used for the calculation of depth to the sources. The depth estimates were obtained for structural index 0 which represents magnetic contacts. It is assumed that there will be a large susceptibility difference across magnetic contacts which causes magnetic anomalies. The window size, depth tolerance and distance tolerance are kept in such a way that the number of depth solutions produced is large and with good clustering. We have used the window sizes ranging from 3 to 10 in the present study and kept the depth and distance tolerance limit below the mean values obtained for each window. Locations where the solutions from all the windows coincide is taken as the final location, other solutions were discarded. In the interpretation of the aeromagnetic data, it is assumed that the long wavelength magnetic sources lie below the base of the sedimentary sequence, since the sediments are considered as nonmagnetic in a general sense. The deeper solutions indicate thicker sedimentary sessions. The magnetic relief observed over sedimentary basins are mostly controlled by the lithology of the basement than by its topography (Alagbe 2015). In the regions where igneous and metamorphic rocks are predominant, the magnetic variations will be complex and deeper features frequently get disguised by the effects of near surface anomalies (Alagbe 2015).

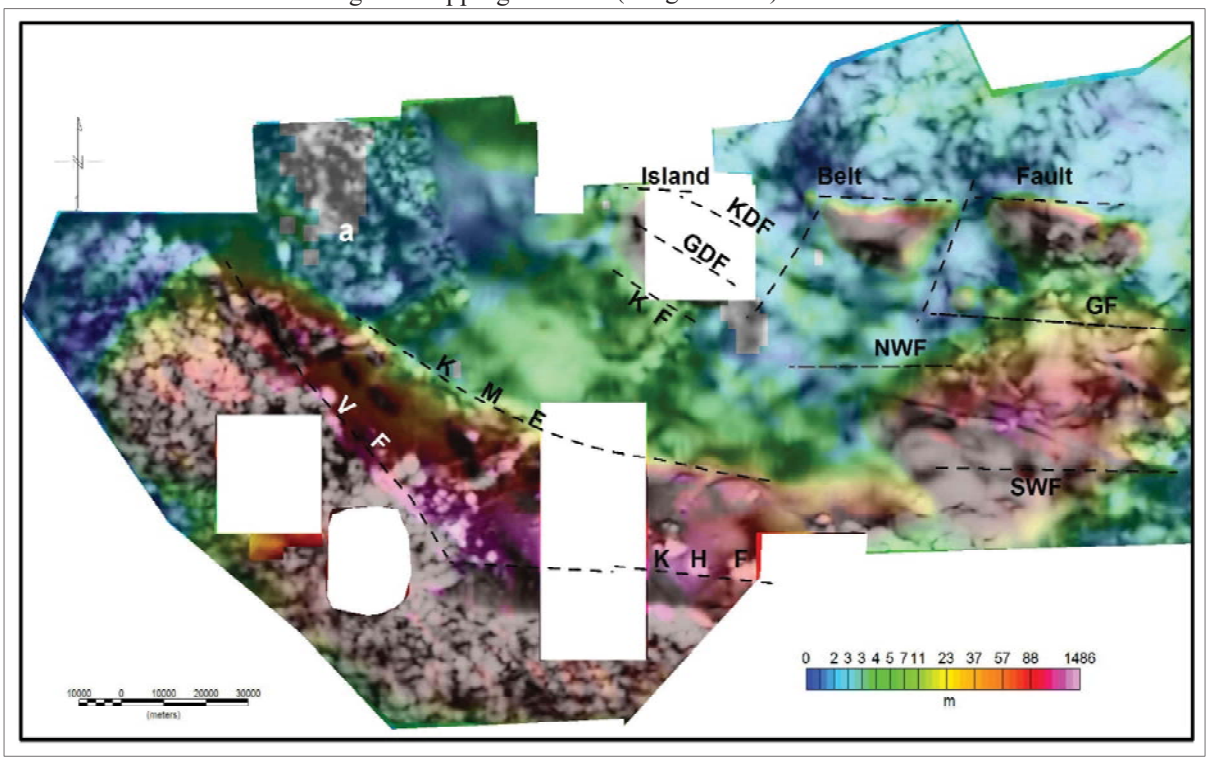

Fig. 3. The analytic signal map draped on the digital elevation model from the SRTM data. Mapped surface faults from Fig.1 is superposed. For abbreviations refer Fig.1.

Euler solutions for a representative window length 3 and SI=0 is superposed on the crustal anomaly map (Fig.2). Depth estimation & edge detection using Euler deconvolution is performed on differential reduction to pole grid which was upward continued to 5km to remove the effect from near surface sources, especially to remove the effects of the trap flows. Hence the depths calculated from Euler deconvolution is used for relative matching and we are not giving weightage to the absolute values. The depth estimation and edge detection carried out using Euler 3D, analytic signal and HGM methods are compared to obtain more meaningful results. These are shown in Fig.4 in which the contact locations picked from all these methods is represented in different colours. The edges/contact identified from HGM maxima are represented in maroon (major) and blue (minor), analytic signal as green and Euler deconvolution solutions in red colours respectively. From this map (Fig.4), we have mapped the major and intermediate lineaments which along with the delineated major magnetic sources at shallow levels (mainly theollitic flows) is used to generate an interpreted map (Fig.5). Major geologic units and mapped faults (from Fig.1) is also included in Fig.5. The major trend of the anomalous features is NW-SE along with secondary structures trending in E-W and NE-SW directions. The western and northwestern part of the study area is complex and show wide variety of trends including several minor lineaments. Other regions where several minor lineaments are observed is the Wagad Uplift (region between south Wagad and Gedi fault in the figure) and north of the Island Belt Fault. Below we discuss some of the observed major and intermediate lineaments some of which lack any surface expression and not been mapped previously. We have represented these lineaments as L1 to L14. The major faults mapped at the surface along with the geology map are also superposed on the interpreted map (Fig.5). The signatures of the mapped major faults like, Kutch Mainland Fault, Katrol hill Fault, Vigodi Fault, Island Belt Fault, and South Wagad Fault are evident. The lineament L1, lying in the south western part of the map, having an E-W trend partly coincides with the Jakhau - Mundra Fault (JMF), a hidden fault identified from electrical imaging (Sastry et al, 2007). L1 is deeper on the west and comparatively shallower on the east as its signature is reflected in the analytic signal peak which enhances shallow sources. The lineament L2 which is lying south of the Katrol Hill fault appears to be a major contact which limits the trap flows to the north. This lineament runs from surface to deeper levels as it shows signature both analytic signal as well as HGM. The lineament L3 coincides with the Katrol Hill Fault (KHF). It appears that L3 turns northeast and does not have any surface expression. Most of the previous studies including seismic, MT etc. were carried out along profiles parallel to the northward extension of L3 hence further studies are required

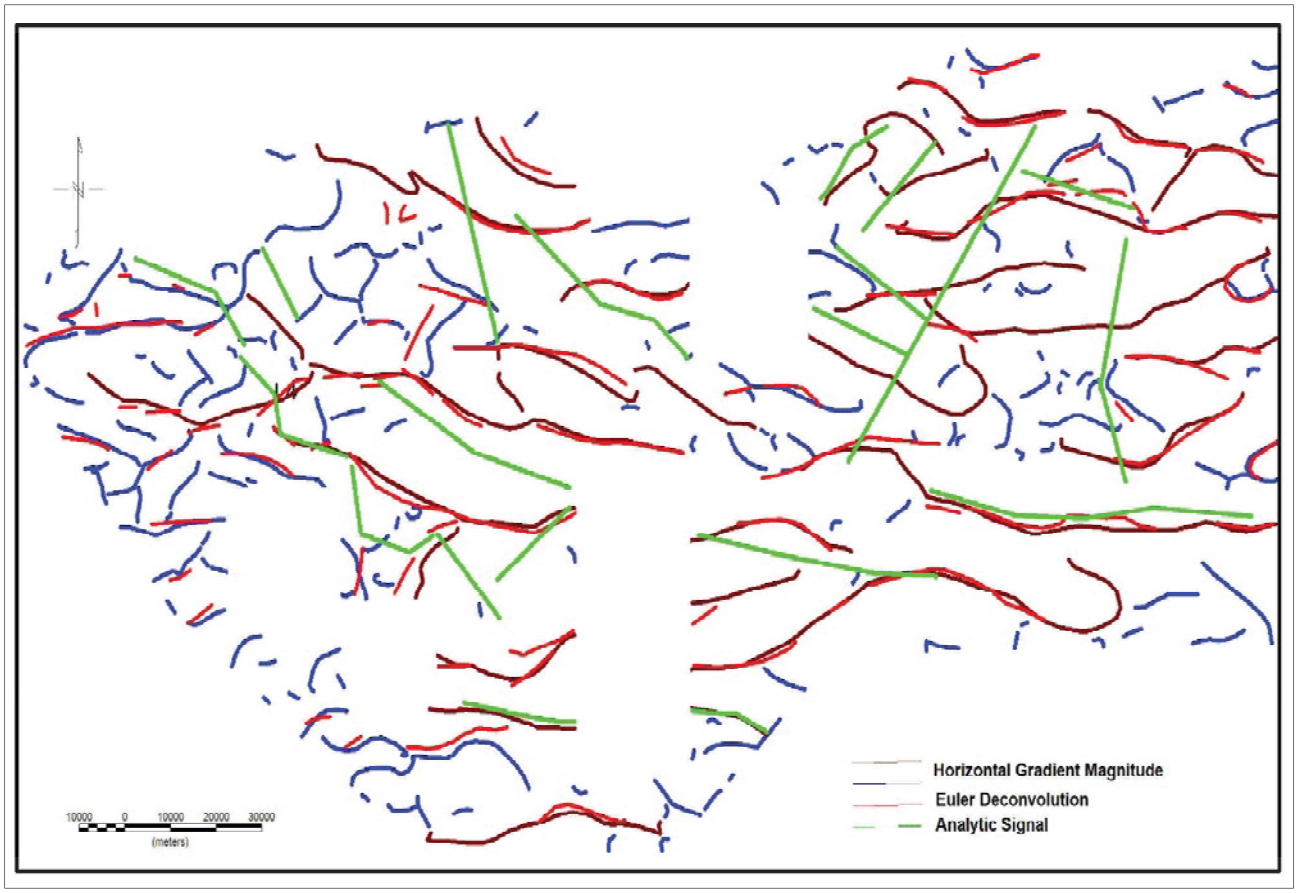

Fig. 4. Comparison of magnetic contact locations derived using HGM (maroon- major lineaments, blue- minor ones), Analytic signal method (green), and Euler deconvolution solutions (Red).

to confirm this inference. The lineament L4, within the Kutch Mainland, having signature both in HGM and Euler deconvolution does not have any surface expression. The region between L4 and Kutch Mainland Fault, Kutch mainland Unit comprising exposed Mesozoic sediments, is characterized by subdued magnetic anomalies and devoid of any major magnetic sources. One important observation is the signature related to KMF, shown as dotted lines in Fig.5, is evident only in the analytic signal (shallow) but not in either HGM or Euler solutions. The lineament L5 runs parallel to the KMF but shifted towards north in the Banni basin but joins the mapped KMF in the southeast. Previous studies have suggested that KMF is north dipping (Biswas 2005) deep seated fault involving the basement and probably Moho. It may be possible that L5 within the Banni basin is the signature of KMF at depth and dipping north. Signature of the geologically mapped South Wagad Fault is evident in shallow (analytic signal) as well as deeper levels (HGM & Euler) as EW trending lineament L6. The signature of L6 can be traced within the Banni basin. It is worth mentioning that L6 does not show any signature in the analytic signal map (shallow) within the Banni basin, where this lineament is overlain by thick sedimentary cover. However analytic signal shows a clear expression of L6 in the east where it is exposed and previously mapped. Hence we interpret that L6 is a major fault involving the basement which might have played a pivotal role in the formation of the Kutch Rift basin. NW-SE lineament, L7 when extended northwest coincides with the NW-SE trending Goradongar Fault (GDF) (Ngangom & Thakkar, 2016)) exposed in the Patcham islands. It appears that this lineament extends further northwest underneath the Rann of Kutch. In addition several other lineaments trending in EW, NW-SE and NE-SW (L8, L9, L10, L11), probably involving the basement, is observed in the region between exposed South Wagad Fault and Island Belt Fault (L10). Island Belt fault (L12) shows in both shallow and deeper levels and appears as to be dislocated rather than a straight fault.

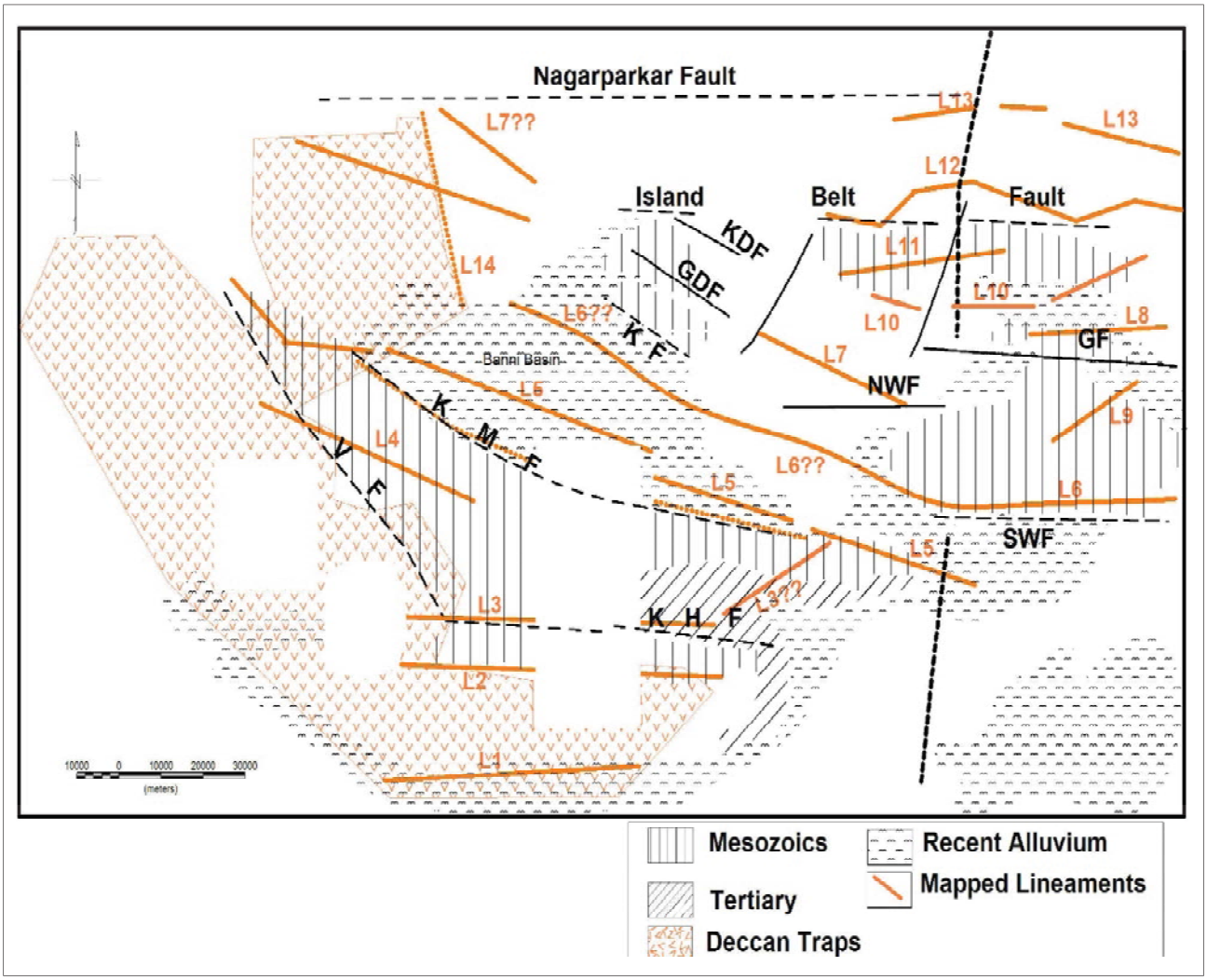

Fig. 5. The major lineaments and magnetic source (basaltic flows) mapped from the analysis of aeromagnetic data using edge detection techniques and analytic signal superposed on the geology and tectonic map of the Kutch Rift basin. For abbreviations and legend refer Fig.1. Thick black dashed line is the Lathi-Rajkot lineament mapped from remote sensing data.

Further north of IBF there is another EW trending lineament L13. The lineament L14 trending in the NNW-SSE direction, traced from analytic signal, is the lithologic contact between the basaltic flows and the Banni sediments. From the central part to the eastern part of the basin, most of the features show E-W trend which agrees with the general trend of the basin architecture. The lineaments L7, L8, L9, L10, L11& L13 have no surface expressions and they are lying underneath the salt plains of Rann of Kutch. The black dotted line represents the NS trending Lathi-Rajkot lineament traced from the satellite imageries. This lineament has been interpreted as a pre-Mesozoic lineament that got reactivated during Tertiary times (Bakliwal & Ramasamy, 1982). It can be seen from Fig.5 that by and large the lineaments delineated from the aeromagnetic data changes its orientation from NW-SE to EW, east of the NS trending Lathi-Rajkot lineament.

The major lineaments discussed above may be related to the tectonic history of the Kutch Rift basin, and may represent faults, axial trace of regional folds and group / formational boundaries. The randomly oriented minor lineaments, maximum in number, with varying distribution, may represent expressions of faults, fractures, dykes and axial traces of large scale folds. The NW-SE trends in the western region changing to EW in the eastern region dominate the inferred lineaments probably involving the basement as well as intra-sedimentary layers. This is in conformity with the structural feature and the trend that resulted from tectonic deformation causing rifting in the Kutch Basin. The most dominant trend (NW-SE) observed in many parts of the study area has been suggested to be intimately associated with the stress history and that has existed since the early Precambrian. The observed correlation between the locations of the basement and intra-sedimentary faults, at places, strongly suggests a tectonic link between the basement and the overlying sedimentary column suggesting reactivation of these faults at different periods during the evolution of the basin. This continued process of reactivation and propagation might have given rise to additional set of faults and fractures (mapped minor lineaments) due to local structural and tectonic disturbances. The general consistency in orientations among the Precambrian basement faults, the lineaments interpreted from aeromagnetic data, and the previously mapped surface faults indicates that the systematic fault system at basement in the area probably have been reactivated many times and thus have connectivity upward perhaps all the way to the surface. Kutch basin has a complicated tectonic regime which is caused either by its formation mechanism or significant tectonic activities that occurred later. To complement the current studies related to the structure of the Kutch Rift Basin, we plan to undertake a detailed examination of the aeromagnetic data integrating with other geophysical and well data to understand the tectonic framework of the Kutch Rift basin.

Summary and Conclusion

Semi-detailed high resolution aeromagnetic data collected over the Kutch rift basin was analyzed to throw light on the major, intermediate and minor lineaments in the study area. The basin is characterized by long to moderate wavelength anomalies with varying amplitudes suggesting presence of mafic to ultramafic magnetic sources at different depth levels. The interpretation of the crustal magnetic anomaly map revealed the dominant trend of the anomalies to be in the NW-SE and E-W directions which agrees with the general trend of the basin. In addition there are secondary anomalies which trend in NE-SW direction. The Banni basin, covered by Tertiary sediments & salt panes, displays long wavelength anomalies, indicating the presence of thick sediments and deeper sources. High frequency anomalies present in the south and southwestern part of the basin indicate the presence of trap flows beneath the exposed sediment cover. One important finding is the presence of trap flows to the northwest of Kutch Mainland Fault which has not been previously reported. In the present study, different edge detection techniques like analytic signal method, horizontal gradient magnitude and Euler 3D are collectively used for the demarcation of the magnetic/lithologic boundaries. The analytic signal made the high frequency anomalies clearer and sharper and brought the indistinct anomalies in to focus. The locations of the magnetic lineaments (which may represent contacts, faults or fractures) are mapped by comparing the HGM, Euler 3D and analytic signal. The signatures of the major faults in the region are well observed and mapped in the present study. The lineaments which are not exposed or previously mapped are demarcated from the examination of the data which add information to the basin architecture. Based on the edge detection techniques we have identified fourteen major and intermediate lineaments of which very few have surface expressions. Some of the identified lineaments are in the subsurface below the sediment cover or the Rann of Kutch and were therefore not delineated. Many of these lineaments may represent basement related faults that have played a pivotal role in the formation of the Kutch basin and may have been reactivated many times in the past and may have connectivity up to the surface. Further analysis and modelling of the aeromagnetic anomalies constrained by geological and geophysical data will provide better insights into the evolution and resource potential of this Mesozoic basin.

Acknowledgements

We thank the Director, Indian Institute of Geomagnetism, Mumbai, for his support and permission to publish this work.

References

Alagbe, O.A., 2015. Depth Estimation from Aeromagnetic Data of Kam. Int. J. Adv. Res. Phys. Sci. 2, 37–52.

Alagbe, O.A. 2, Sunmonu, L.A., 2014. Interpretation of Aero magnetic Data from Upper Benue Basin, Nigeria Using Automated Techniques. IOSR J. Appl. Geol. Geophys. 2, 22–40.

Arkani -Hamed, J., 1988. Differential reduction-to-the-pole of regional magnetic anomalies. Geophysics, 53, 1592-1600.

Bakliwal, P.C. and Ramasamy, S.M. 1985. Occurrence of circular features in parts of Thar desert, Rajasthan. J. Geol. SOC.India, 26, 77-86.

Bemsen, I.E., Bemsen, I.E., Godwin, O.A., Kenechukwu, A.E., Ifeanyi, C.A., Ojonugwa, U.A., Chukwunonso, O.C., 2013. Spectral Analysis of Aeromagnetic Data over Part of the Southern Bida basin, West-Central Ni geria. IJFPS 3, 27–31.

Betts, P.G., Giles, D & Lister, G.S. 2004. Aeromagnetic pat terns of half-graben and basin inversion: implications for sediment-hosted massive sulfide Pb–Zn–Ag explo ration. Journal of Structural Geology, 26, 1137–1156

Biswas, S.K., 2005. SPECIAL SECTION : INTRAPLATE SEISMICITY A review of structure and tectonics of Kutch basin , western India , with special reference to earthquakes. current science 88, 10-25.

Biswas, S.K., 1999. a review on the evolution of rift basins in india during gondwana with special reference to west ern indian basins and their hydrocarbon prospects. PINSA 65, 261–283.

Biswas, S.K., 1987. Regional tectonic framework, structure and evolution of the western marginal basins of India. Tectonophysics 135, 307–327.

Blakely, R.J., 1995. Potential theory in Gravity and Mag netic applications. Cambridge University Press, Aus tralia

Chandrasekhar, D. V., Mishra, D.C., 2002. Some geodynamic aspects of Kutch basin and seismicity: An insight from gravity studies. Curr. Sci. 83, 492-498

Cooper, G.R.J., Cowan, D.R., 2005. Differential reduction to the pole. Comput. Geosci. 31, 989–999.

Grant, F.S. 1985. Aeromagnetics geology and oreenvirone ments, I. Magnetite in igneous, sedimentary and meta morphic rocks: An overview. Geoexploration 23, 03-333.

Grauch ,V.J.S. & Hudson ,M. R. 2007. Guides to understand ing the aeromagnetic expression of faults in sedimen tary basins: Lessons learned from the central Rio Grande rift, New Mexico. Geosphere, 3, 596–623.

Grauch, B.V.J.S., Drenth, B.J., 2009. High-Resolution Aero magnetic Survey To Image Shallow Faults , Poncha Springs and Vicinity , Chaffee County, Colorado.U.S. Geological survey Open-file Report 2009-1156,31 p.

Gunn, P.J., Maidment, D., Milligan, P., 1997. Interpreting aeromagnetic data in areas of limited outcrops - part 2. AGSO J. Aust. Geol. Geophys. 17, 175–185.

Kayal, J.R., Mukhopadhyay, S., 2006. Seismotectonics of the 2001 Bhuj earthquake (Mw 7 . 7) in western India : Constraints from aftershocks. J.Ind. Geophys. Union 10, 45–57.

Karanth R.V., Gadhavi M.S., 2007. Structural intricacies: Emergent thrusts and blind thrusts of central Kutch, Western India. Current Science, 93, 1271-1280

Karmalkar, N.R., Sarma, P.K., 2003. Characterization and origin of silicic and alkali-rich glasses in the Upper mantle-derived spinel peridotite xeno- liths from alkali basalts , Deccan Trap , Kutch , northwest India. Current Science 85, 386-392.

Kishore, R.K., Rao, C.R., 2004. Basement characteristics of Papaghni Basin of Eastern Dharwar Craton (Inida) - An inference from Aeromagnetic study. 8, 311–317.

Kumar,M.K., G.P., Chaudhary, P., Choudhary, V.K., Nagar, M., Khuswaha, D., Patel, P., Gandhi, D., Rastogi, B.K., 2017. Geothermics Magnetotelluric investigations to identify geothermal source zone near Chabsar hotwater spring site , Ahmedabad , Gujarat , Northwest India. Geothermics 65, 198–209.

Lu, R.S., Mariano, J., Willen, D.E., 2003. Differential reduction of magnetic anomalies to the pole on a mas sively parallel computer. Geophysics 68, 1945–1951.

MacLeod, I.N., Jones, K., Dai, T.F., 1993. 3-D analytic signal in the interpretation of total magnetic field data at low magnetic latitudes. Explor. Geophys. 24, 679-688.

Milligan, P.R. & Gunn, P.J., 1997. Enhancements and presentation of airborne geophysical data. AGSO Journal of Australian Geology & Geophysics, 17(2), 63-75.

Nabighian, M. N., 1984. Towards a three-dimensional automatic interpretation of potential field data via generalized Hilbert transforms - Fundamental relations. Geophysics, 47, 780-786

.

Nabighian, M. N., Grauch, V. J. S., Hansen, R. O., LaFehr, T. R., Li, Y., Peirce, J. W., Phillips, J. D. and Ruder, M. E. 2005. The historical development of the magnetic method in exploration. Geophysics 70, 33-61.

Ngangom, M., Thakkar, M.G., 2016. Morphometric Characterization and Neotectonic Evolution of Island publication of the Geological Scociety of India 151-167

Phillips, J. D., Saltus,R.W. and Reynolds,R.L. 1998. Sources of Magnetic Anomalies over a Sedimentray Basin: Preliminary Results from the Coastal Plains of the Artic National Wildlife Refuge, Alaska. In. Geologic Applications of Gravity and Magnetics: Case Histories. Spl. Publ. Society of Exploration Geophysicists and American Association of Petroleum Geologists, 130-134.

Prasad, B.R., Venkateswarlu, N., Prasad, A.S.S.S.R.S., Murthy, A.S.N., Sateesh, T., 2010. Basement configuration of on-land Kutch basin from seismic refraction studies and modeling of first arrival travel time skips. J. Asian Earth Sci. 39, 460-469.

Rajaram, M, Anand,S.P. &.Erram,V.C. 2000. Magnetic studies over Krishna-Godavari basin in Eastern Continental margin of India, Gondwana Research, 3, 385-393.

Rajaram, M. & Anand, S.P. 2014. Aeromagnetic signatures of Precambrian shield and suture zones of Peninsular India. Geoscience Frontiers, 5, 3–15

Reeves C. V., 2005. Aeromagnetic Surveys, Principles, Practice and Interpretation; Geosoft, 155

Reid, A.B., Allsop, J.M., Granser, H., Millet, A.J., Somerton, I.W., 1990. Magnetic interpretation in three dimensions using Euler deconvolution. Geophysics 55, 80-91.

Roest, W.R., Verhoef, J., Pilkington, M., 1992. Magnetic interpretation using the 3-D analytic signal. Geophysics 57, 116–125.

Seshu, D., Rama Rao, P., Naganjaneyulu, K., 2016. Three-dimensional gravity modelling of Kutch region, India. J. Asian Earth Sci. 115, 16–28.

Silva, J.B.C., 1986. Reduction application to the pole as an inverse to low-latitude anomalies problem and its application to low-latitude anomalies. Geophysics 51, 369–382.

Singh, V.P., Shanker, D., Singh, H.N., Banerjee, M., 2007. Upper mantle instability and seismic activity of Kutch and adjoining areas with special reference to Bhuj earthquake of 2001, Gujarat, India - A petrologic model. Acta Geod. Geophys. Hungarica 42, 323–340.

Thompson, D.T., 1982. EULDPH: A new technique for making computer-assisted depth estimates from magnetic data. Geophysics 47, 31-37.